

Aluminum incorporation into AlGa_N grown by low-pressure metal organic vapor phase epitaxy

G. S. Huang, H. H. Yao, T. C. Lu, H. C. Kuo, and S. C. Wang

Citation: *Journal of Applied Physics* **99**, 104901 (2006); doi: 10.1063/1.2199972

View online: <http://dx.doi.org/10.1063/1.2199972>

View Table of Contents: <http://scitation.aip.org/content/aip/journal/jap/99/10?ver=pdfcov>

Published by the [AIP Publishing](#)

Articles you may be interested in

[Diffusion of Mg dopant in metal-organic vapor-phase epitaxy grown GaN and Al_xGa_{1-x}N](#)
J. Appl. Phys. **113**, 073514 (2013); 10.1063/1.4792662

[Relaxation and critical strain for maximum In incorporation in AlInGa_N on GaN grown by metal organic vapour phase epitaxy](#)
J. Appl. Phys. **112**, 093524 (2012); 10.1063/1.4764342

[Strain effects on the intersubband transitions in GaN/AlN multiple quantum wells grown by low-temperature metal organic vapor phase epitaxy with AlGa_N interlayer](#)
Appl. Phys. Lett. **95**, 161908 (2009); 10.1063/1.3253715

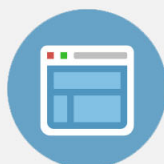
[Indium migration paths in V-defects of InAlN grown by metal-organic vapor phase epitaxy](#)
Appl. Phys. Lett. **95**, 071905 (2009); 10.1063/1.3204454

[Oxygen induced strain field homogenization in AlN nucleation layers and its impact on GaN grown by metal organic vapor phase epitaxy on sapphire: An x-ray diffraction study](#)
J. Appl. Phys. **105**, 033504 (2009); 10.1063/1.3074095



Re-register for Table of Content Alerts

Create a profile.



Sign up today!



Aluminum incorporation into AlGa_xN grown by low-pressure metal organic vapor phase epitaxy

G. S. Huang,^{a)} H. H. Yao, T. C. Lu, H. C. Kuo, and S. C. Wang

Department of Photonics & Institute of Electro-Optical Engineering, National Chiao Tung University, 1001 TA Hsueh Road, Hsinchu, Taiwan 300, Republic of China

(Received 20 June 2005; accepted 3 April 2006; published online 24 May 2006)

Aluminum (Al) incorporation in Al_xGa_{1-x}N films grown by low-pressure metal organic vapor phase epitaxy using trimethylaluminum (TMAI) and trimethylgallium as group III precursors has been systematically studied. The solid phase Al composition of the Al_xGa_{1-x}N films varied nonlinearly with the Al gas phase composition. The incorporation kinetics of Al_xGa_{1-x}N alloy has been analyzed by using an adsorption-trapping model. Two parameters were used to characterize the properties of Al incorporation, i.e., the capture radius and the adsorption time of Al atoms. An exponential function of the Al composition of the Al_xGa_{1-x}N films versus the TMAI gas flow rate was obtained. It was demonstrated that the adsorption time of the Al atom was larger than the growth time of one atomic layer. The effects of ammonia flow rate, crystal growth rate, and growth temperature on the adsorption parameters were also discussed. © 2006 American Institute of Physics.

[DOI: [10.1063/1.2199972](https://doi.org/10.1063/1.2199972)]

I. INTRODUCTION

AlGa_xN and AlGa_xN/GaN heterostructures and multiple quantum wells have been recognized as important materials for high-temperature/high-power/high-frequency electronic and optoelectronic devices, e.g., heterostructure field-effect transistors,^{1,2} ultraviolet light emitting diodes,³ ultraviolet laser diodes,⁴⁻⁶ and terahertz quantum cascade lasers.⁷ For realization of these devices, it is necessary to control the aluminum (Al) composition in the solid phase of AlGa_xN films and optimize growth conditions for high quality AlGa_xN films. Al incorporation into ternary semiconductor compounds such as Al_xGa_{1-x}N during metal organic vapor phase epitaxial (MOVPE) growth has been studied.⁸⁻¹⁰ Kondratyev *et al.* reported an Al composition saturation upon the excessive supply of Al precursor at a growth pressure of 400 mbar, which was an evidence that all the additional trimethylaluminum (TMAI) was converted into particles, giving no increase of the AlN growth rate.⁸ However, the Al composition increased almost proportionally with the increase of the TMAI flow rate at a growth pressure of 100 mbar.⁸ In order to avoid periodically switching from moderate growth pressure for GaN to low growth pressure for AlGa_xN, when growing AlGa_xN/GaN multiple quantum wells and superlattices, one should choose the growth pressure in a suitable way for both layers. In this report, although we chose the growth pressure at 133 mbar between 400 and 100 mbar, the Al/gallium (Ga) solid composition ratio of Al_xGa_{1-x}N did not change linearly with the Al/Ga gas phase ratio in MOVPE growth even when other growth parameters were kept constant. During the deposition of Al_xGa_{1-x}N ternary layers, the surface kinetics might play a key role in determining the Al solid composition. The effects of growth conditions on the Al incorporation have not been studied

systemically. We have performed a detailed study on the growth conditions for controlling the Al composition of Al_xGa_{1-x}N films at this growth pressure (133 mbar) in order to obtain high performance AlGa_xN/GaN multiple quantum wells and superlattices. A surface-adsorption-trapping model^{11,12} was used to describe the Al solid composition in the films versus the gas phase composition of TMAI/(TMAI+TMGa). The effects of V/III ratio and growth temperature on the adsorption parameters were also discussed.

II. EXPERIMENTAL PROCEDURE

All the samples in this work were grown in a low-pressure vertical-type EMCORE D75 reactor with a high-speed rotational susceptor. The reagents were pure ammonia, TMGa, and TMAI. The purified hydrogen and nitrogen were used as the carrier gases. The reactor pressure and rotating speed were 133 mbar and 900 rpm, respectively. *C*-plane sapphire epitaxial substrates were used for all the growth.

The group III and V precursors were separated in two manifolds and entered the reactor, respectively. Prior to material growth, the sapphire substrate was annealed to remove any residual impurity on the surface in H₂ ambient at 1100 °C for 5 min. For all samples, a normal 30-nm-thick GaN nucleation layer was grown on the substrate at 500 °C, followed by a 2- μ m-thick GaN layer and a 0.4- μ m-thick AlGa_xN film. The first group of samples was grown by varying the TMAI flow rate from 3 to 18 SCCM (SCCM denote cubic centimeter per minute at STP) with the TMGa flow rate of 6 SCCM and NH₃ flow rate of 600 SCCM. The second group of samples was grown by varying the NH₃ flow rate from 300 to 1200 SCCM with the TMGa flow rate of 6 SCCM and TMAI flow rate of 5 SCCM. The AlGa_xN growth temperature was 1110 °C for the above two groups of samples. The third group of samples was grown at different growth temperatures from 1050 to 1110 °C with the

^{a)}Author to whom correspondence should be addressed; electronic mail: gshuang@mail.nctu.edu.tw

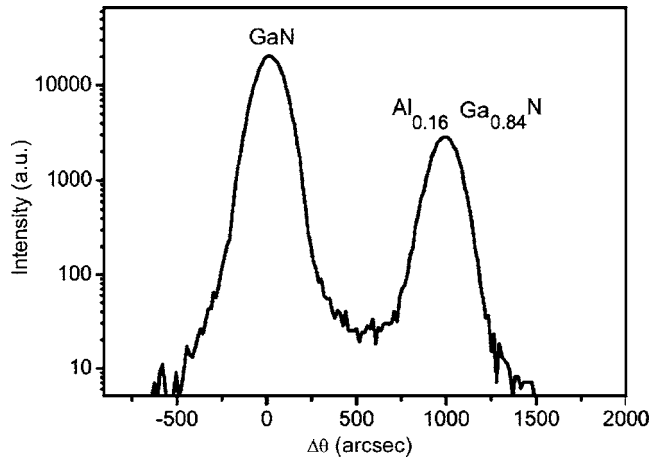


FIG. 1. XRD rocking curve (0004) of $\text{Al}_x\text{Ga}_{1-x}\text{N}$ film grown on GaN/sapphire substrate.

TMGa flow rate of 6 SCCM, TMAI flow rate of 5 SCCM, and NH_3 flow rate of 600 SCCM. All samples were grown using a constant total flow of H_2 and N_2 carrier gases and the ratio of H_2/N_2 was constant. The growth processes were *in situ* monitored by using the filmetrics F-series thin-film measurement system. The thickness was measured by scanning electron microscope (SEM) (JEOL JSM-7000F) and the measurement accuracy was 3.0 nm. The compositions and lattice parameters of $\text{Al}_x\text{Ga}_{1-x}\text{N}$ films on GaN were measured by using a Bede Scientific D1 double crystal x-ray diffraction (XRD).

III. RESULTS AND DISCUSSION

Figure 1 shows the double crystal XRD of an $\text{Al}_x\text{Ga}_{1-x}\text{N}/\text{GaN}$ sample. The Al composition x of $\text{Al}_x\text{Ga}_{1-x}\text{N}$ film can be calculated by

$$x = \frac{c_{\text{GaN}}}{c_{\text{GaN}} - c_{\text{AlN}}} \left(\frac{\sin(\theta_B + 2\Delta\theta)}{\sin \theta_B} - 1 \right), \quad (1)$$

where $c_{\text{GaN}} = 5.185 \text{ \AA}$, and $c_{\text{AlN}} = 4.798 \text{ \AA}$ are the bulk lattice constants of GaN and AlN, respectively, $\Delta\theta$ is the diffraction angle separation between AlGa_xN and GaN peaks, and θ_B is the Bragg angle of the GaN (0004). Because the thickness of epilayer was about 0.4 μm , the strain in $\text{Al}_x\text{Ga}_{1-x}\text{N}$ film had been relaxed completely. The Al composition of this $\text{Al}_x\text{Ga}_{1-x}\text{N}$ film was found to be 0.16. The full widths at half maximum (FWHM) of GaN and AlGa_xN were 146 and 148 arc sec, respectively. These results indicated good qualities of these layers.

Figure 2 shows the measured Al composition of the $\text{Al}_x\text{Ga}_{1-x}\text{N}$ epilayers varying with gas phase composition ξ , which is the TMAI gas mole fraction over TMAI and TMGa. The gas mole fraction of one source was obtained by calculation of the partial pressure and flow rate of the source at the set temperature. When ξ increased from 0.08 to 0.49, x increased from 0.10 to 0.27. At first, the Al solid composition was larger than the gas phase composition and then the Al solid composition was nearly same as the gas phase composition when ξ increased to 0.21. When ξ increased to 0.49, the Al solid composition became saturated. Choi *et al.* also

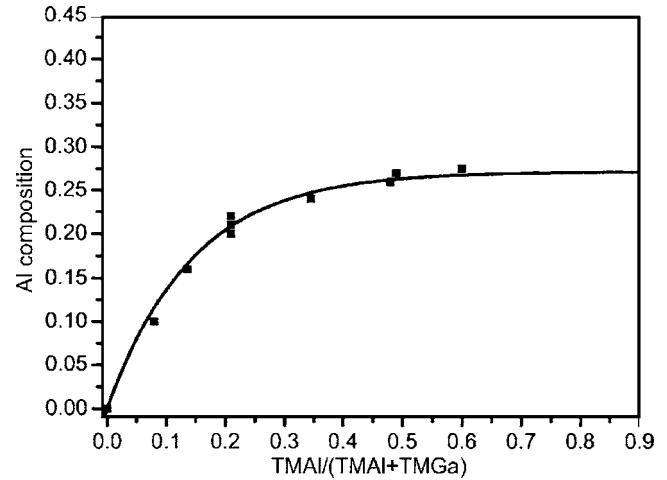


FIG. 2. Measured Al composition x vs TMAI source flow composition in group III gas mixture ratio ξ . It shows that the Al composition saturated at $\xi = 0.4$ when the $\text{Al}_x\text{Ga}_{1-x}\text{N}$ epilayers were grown at 1110 °C. The solid curve is a theoretical fit by using Eq. (8).

reported that Al solid composition did not increase linearly with increasing the Al gas composition but saturated to the Al solid composition of 0.2 under the growth pressure of 200 mbar.¹⁰ This Al incorporation into MOVPE growth of $\text{Al}_x\text{Ga}_{1-x}\text{N}$ films on sapphire substrates by using TMAI and TMGa as the group III sources in hydrogen with nitrogen ambient can be explained by using a surface-adsorption-trapping model.^{11,12}

The AlGa_xN was grown layer-by-layer by successive growth of atomic layers of the group III and V atoms. The alternating group III and V atom planes were aligned with [0001] orientation in the wurtzite structure of AlGa_xN. The plane of group V atom in AlGa_xN crystal structure consists of nitrogen atoms. For a hexagonal lattice structure, the surface atomic density N_s^0 is given by $n/2.6a^2$, where a is the lattice constant and n is the number of atoms per hexagonal cell. The lattice constant of $\text{Al}_x\text{Ga}_{1-x}\text{N}$ film is 3.173 \AA when x is about 0.2 and n is 3; thus we have $N_s^0 = 1.15 \times 10^{15} \text{ cm}^{-2}$. The plane of group III atoms of epilayer consists of Ga and Al atoms. In order to obtain optimal growth conditions, overpressure of group V source was necessary to prevent $\text{Al}_x\text{Ga}_{1-x}\text{N}$ decomposition on the surface during growth. The overpressure of NH_3 as group V source provided a group V stabilized surface and the epitaxial growth rate was controlled by the arrival of group III atoms. Under the assumption that there existed a fixed number of group III adsorption sites on $\text{Al}_x\text{Ga}_{1-x}\text{N}$ surface, the kinetics of group III incorporation during epitaxy were formulated phenomenologically in the following. Two parameters, the capture radius R_c and the adsorption time τ_c , were used to describe the adsorption process during the $\text{Al}_x\text{Ga}_{1-x}\text{N}$ film epitaxial growth.^{11,12} The adsorption-desorption process is schematically shown in Fig. 3. According to this model, NH_3 reacted with the monomethylaluminum (MMAI) and monomethylgallium (MMGa) generated by pyrolysis of TMAI and TMGa to form $\text{Al}_x\text{Ga}_{1-x}\text{N}$ films on the epilayer surface.⁹ In the epitaxial growth, each NH_3 acted as an adsorption center; thus all the MMAI within the region of radius R_c around the adsorption center would be captured. One MMAI reacted with the ad-

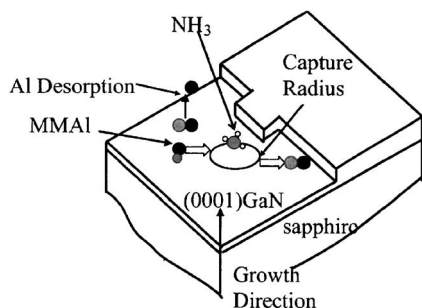


FIG. 3. A schematic diagram showing the Al incorporation process on (0001) $\text{Al}_x\text{Ga}_{1-x}\text{N}$ surface during epitaxial growth.

sorption center to form an AlN particle. Meanwhile the MMGa species also reacted with the adsorption center to form a GaN particle. These particles moved to the kick and step to form an AlGaN layer. For simplicity, we assumed that each adsorption center captured only one MMAI or MMGa molecule. The MMAI molecule diffused onto the epilayer surface. The probability of a MMAI molecule on the surface finding its adsorption center would therefore be proportional to the diffusivity of the MMAI molecule. It meant that the capture radius R_c to the first order should be proportional to the surface diffusivity D_s of MMAI molecules or $R_c = R_0 \exp(-Q_d/kT)$,^{11,12} where Q_d was the activation energy for surface diffusion of MMAI molecules.

The time of adsorption τ_c was defined as the lifetime of the captured MMAI before desorbing from the adsorption center.¹¹ The MMAI incorporation process in each atomic layer during the epitaxial growth could be considered as the terminated adsorption-desorption process in the time interval equal to the growth time of one atomic layer Δt . If $\tau_c \geq \Delta t$, all the captured MMAI would be buried to form the atomic layer. For $\tau_c < \Delta t$, the probability of the captured MMAI to be trapped by the current layer reduced to $\tau_c/\Delta t$. Here we defined a ψ function, which was described as $\psi(\tau_c/\Delta t) = \tau_c/\Delta t$ for $\tau_c < \Delta t$ and $\psi(\tau_c/\Delta t) = 1$ for $\tau_c \geq \Delta t$.¹¹ Therefore if we let N_s^* be the density of the adsorption centers, which could absorb MMAI molecules, N_s the adsorbed MMAI molecules per unit area at time t on the AlGaN (0001) surface, F_i the incoming flux of MMAI molecules, and α the capture coefficient of MMAI molecules, the rate equation could be written as¹¹

$$\frac{dN_s}{dt} = \alpha F_i (N_s^* - N_s). \quad (2)$$

The capture coefficient could be expressed as $\alpha = N_s^*/N_s^0 R_c \psi(\tau_c/\Delta t)$,¹¹ where N_s^*/N_s^0 was the probability for the incident MMAI molecules to hit the adsorption centers. The time of adsorption τ_c could be expressed as $\tau_c = \tau_0 \exp(Q_{des}/kT)$.¹¹ Q_{des} was the activation energy for desorption. It was clear that the capture coefficient had already taken into account the desorption of adsorbed MMAI molecules, and no additional term was needed for desorption. Thus adsorption rate equation could be written as^{11,12}

$$\frac{dN_s}{dt} = \frac{N_s^*}{N_s^0} R_c \psi\left(\frac{\tau_c}{\Delta t}\right) F_i (N_s^* - N_s). \quad (3)$$

For a vertical reactor, the Reynolds number Re for hydrogen and nitrogen carrier gas flow at a mean flow rate u_{in} can be defined as¹³

$$Re = u_{in} r_s \rho / \mu, \quad (4)$$

where r_s is the susceptor radius, ρ is the density of N_2 and H_2 mixture, and μ can be calculated by the dynamic viscosity of N_2 and H_2 . For N_2 and H_2 carrier gas flow at 4.5 l/min and susceptor temperature of 1110 °C, Re was estimated to be ~ 7.30 , which was in the range for laminar flow.¹³ Since the calculated thermal velocity of TMAI molecules at 1110 °C was more than two orders of magnitude higher than the mean flow velocity,¹³ the impinging flux F_i could be calculated directly from the partial pressure using statistical thermodynamics and neglecting the mean flow velocity. Since the TMAI partial pressure was proportional to the TMAI source flow rate f_{Al} and the probability of TMAI impinging flux was inversely proportional to the total flux of group III elements, or $\text{III} = f_{Al} + f_{Ga}$, where f_{Ga} was the TMGa source flow rate, the impinging flux was given by

$$F_i = C \frac{f_{Al}}{\text{III}}, \quad (5)$$

where C was the flux factor which is equal to the number of MMAI molecules impinging on a unit area of substrate surface per 1 SCCM flow of the source gas. Define $\beta = N_s^*/N_s^0 R_c \psi(\tau_c/\Delta t) C$ and $\xi = f_{Al}/\text{III}$ and then the solution of Eq. (3) has a simple form given by

$$N_s = N_s^* (1 - e^{-\beta \xi t}). \quad (6)$$

The adsorption-desorption process for each atomic layer proceeded in only a short time period Δt which was equal to the time interval for the growth of one atomic layer. By substituting Δt into Eq. (6), the Al surface concentration incorporated into the $\text{Al}_x\text{Ga}_{1-x}\text{N}$ film depended on the TMAI gas phase composition ξ :

$$N_s = N_s^* (1 - e^{-\beta \xi \Delta t}). \quad (7)$$

The bulk Al atomic density of the epilayer was $N_{Al} = N_s/d$, where $d = c/2$ was the thickness of one atomic layer and c was the lattice constant of the z axis. The Al solid composition in the epilayer was $x = N_{Al}/N^0$, where N^0 was the number of group III atoms in a unit volume. The surface group III atomic density of epilayer calculated as mentioned $N_s^0 = N^0 c/2$. Thus,

$$x = \frac{N_s^*}{N_s^0} (1 - e^{-\beta \xi \Delta t}). \quad (8)$$

Figure 2 shows that at saturation condition, the probability for the incident MMAI molecules to hit the adsorption centers, N_s^*/N_s^0 , was 0.272, which means that the MMAI molecules were incorporated into 27.2% growth sites of group III during these growth conditions. Equation (8) fits the experimental results quite well as shown in Fig. 2. The average growth time was $\Delta t = 1.31$ s for one atomic layer on (0001) GaN at 1110 °C. Equation (8) therefore reduced to one adjustable parameter β . To demonstrate the agreement between the adsorption-trapping model and the measured data, Fig. 2

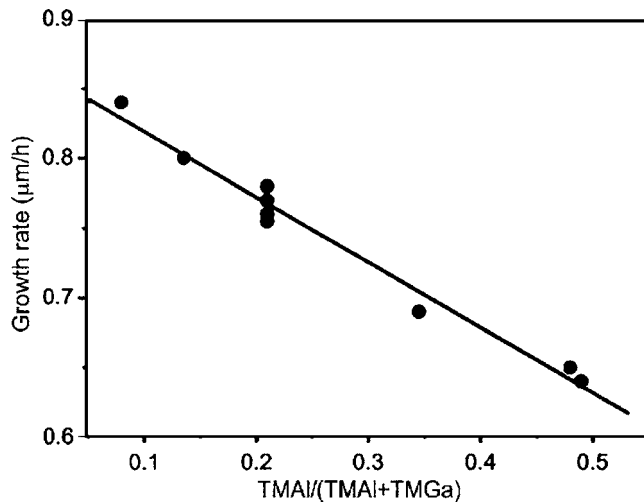


FIG. 4. The growth rate of AlGaIn films with varying TMAI flow rate at NH_3 flow rate of 600 SCCM.

shows an excellent fit with $\beta=5.28$, where β was an incorporation factor which was equal to the number of TMAI molecules adsorbed on a unit area of substrate surface per 1 SCCM flow of the source gas per unit time. At small values of ξ , Eq. (8) reduced to $x=(N_s^*/N_s^0)\beta\xi\Delta t$, which indicated that the Al solid composition was directly proportional to both the TMAI gas phase composition ξ and the time of surface exposure to the source gas between the growth of successive layers, which was inversely proportional to the growth rate. Figure 4 shows the growth rate of $\text{Al}_x\text{Ga}_{1-x}\text{N}$ films with varying TMAI gas phase composition shown in Fig. 2. It confirmed that the growth rate decreased with increasing the Al composition of $\text{Al}_x\text{Ga}_{1-x}\text{N}$ films.

Figure 5 shows the Al composition in solid and growth rate of AlGaIn as a function of NH_3 flow rate. TMAI and TMGa flow rates were fixed at 4.34 and 16.4 $\mu\text{mol}/\text{min}$, respectively. The Al composition in the solid increased with increasing the NH_3 flow rate, meanwhile the growth rate decreased. The increase of NH_3 flow rate meant that the density of the adsorption centers N_s^* increased, which increased the Al incorporation and resulted in an increase of Al solid composition. This agreed with the prediction made in

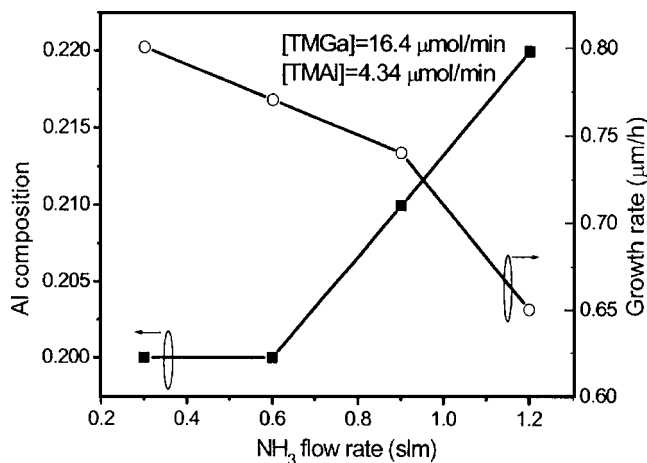


FIG. 5. Al compositions in the solid and growth rate of AlGaIn as a function of ammonia flow rate. TMAI gas composition ξ remained constant at 0.21.

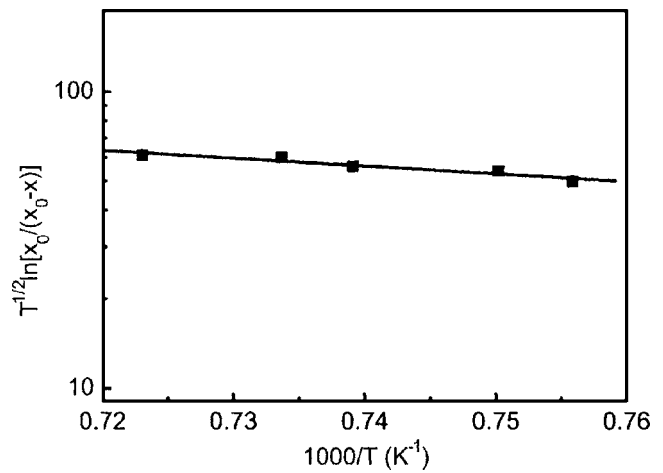


FIG. 6. $\ln\{\sqrt{T}\ln[x_0/(x_0-x)]\}$ vs $1/T$ curve for an $\text{Al}_x\text{Ga}_{1-x}\text{N}$ film grown at different temperatures. A negative slope is seen when $f_{\text{Al}}=5$ SCCM.

Eq. (8). When ξ was more than 0.4, x increased slowly with ξ . At surface saturation composition, the second term in Eq. (8) approached to zero and $x \approx N_s^*/N_s^0$. Thus N_s^* determined the Al solid composition of $\text{Al}_x\text{Ga}_{1-x}\text{N}$ films. When the growth pressure decreased to 66 mbar, the high Al solid composition of $\text{Al}_{0.6}\text{Ga}_{0.4}\text{N}$ films was obtained. This result showed that the density of adsorption centers N_s^* increased with the growth pressure, meanwhile β increased with N_s^* .

Let $x_0=N_s^*/N_s^0$. Then Eq. (8) could be written as

$$x = x_0(1 - e^{-\beta\xi\Delta t}), \quad (9)$$

where $\beta\Delta t$ was given by

$$\beta\Delta t = x_0 R_c \psi(\tau_c/\Delta t) C \Delta t = \begin{cases} x_0 R_0 \tau_0 e^{(Q_{\text{dec}}-Q_d)/kT} C & \text{for } \tau_c < \Delta t \\ x_0 R_0 e^{-Q_d/kT} C \Delta t & \text{for } \tau_c \geq \Delta t. \end{cases} \quad (10)$$

Since Q_{des} was larger than Q_d , temperature dependences of $\beta\Delta t$ would be different for $\tau_c < \Delta t$ and $\tau_c \geq \Delta t$.¹¹

The flux factor C could be expressed as¹⁴

$$C = \frac{1}{4} n \nu = \frac{1}{4} n \sqrt{\frac{8kT}{\pi M}}, \quad (11)$$

where ν was the mean thermal velocity, M was the molecular weight of TMAI, and n was the density of TMAI molecules in the gas flow. Assuming that the gas temperature T right above the substrate was the same as the substrate temperature, n was inversely proportional to T due to expansion.¹¹ Therefore, C was proportional to $1/\sqrt{T}$. At low TMAI source flow rate, the activation energy for surface diffusion Q_d can be obtained by plotting $\ln\{\sqrt{T}\ln[x_0/(x_0-x)]\}$ vs $1/T$ from Eq. (9) as shown in Fig. 6 for $f_{\text{Al}}=5$ SCCM. The negative sign of the slope confirmed that the time of adsorption τ_c was more than Δt . The Q_d can be calculated from the slope of curve $Q_d=0.53$ eV. The β increased with growth temperature from Eq. (10).

When $\xi > 0.4$, Eq. (8) reduced to $x=N_s^*/N_s^0$; x became temperature independent. For $\xi < 0.4$, the temperature dependence of x decreases monotonically with increasing f_{Al} . In this case, x had a complicated relationship with temperature. Figure 7 plots the measured x vs T with different f_{Al} values.

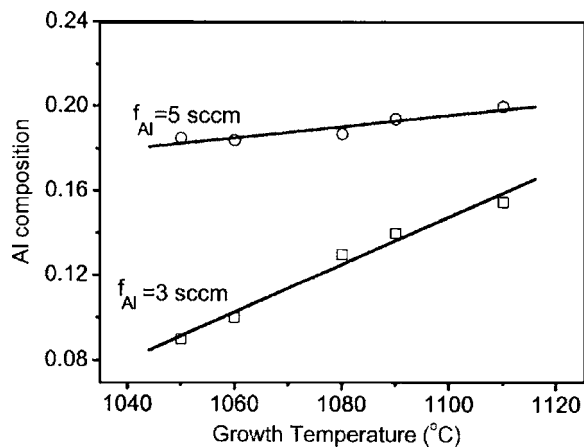


FIG. 7. Temperature dependence of the Al composition in $\text{Al}_x\text{Ga}_{1-x}\text{N}$ films for two Al source flow rates at flow rates of 3 and 5 SCCM, respectively. It shows that with an increase in TMAI flow rate f_{Al} , the Al composition in the film becomes less temperature dependent.

It was observed that the slope of x vs T decreased as f_{Al} increased. This indicated that the Al composition x of $\text{Al}_x\text{Ga}_{1-x}\text{N}$ films became less temperature dependent on f_{Al} . This agreed with the prediction made in Eq. (8).

IV. CONCLUSIONS

Aluminum incorporation during MOVPE growth of $\text{Al}_x\text{Ga}_{1-x}\text{N}$ films by using TMGa and TMAI as group III sources in N_2 and H_2 ambient was investigated both experimentally and theoretically. The Al composition in solid phase measured from XRD was plotted as a function of gas phase compositions ξ . It was found that the Al composition increased with ξ when ξ was below 0.4 and became saturated when the gas phase composition was above 0.4. A theoretical model based on MMAI surface adsorption trapping was proposed to explain experimental results based on the kinetics of Al incorporation during the $\text{Al}_x\text{Ga}_{1-x}\text{N}$ MOVPE growth. Two parameters, the capture radius R_c and desorption time τ_c for MMAI molecule, were used to characterize the surface adsorption center for MMAI molecule. The analysis showed that the Al composition of $\text{Al}_x\text{Ga}_{1-x}\text{N}$ film was a function of the gas phase composition ξ during the MOVPE growth. The

Al saturation composition of $\text{Al}_x\text{Ga}_{1-x}\text{N}$ film corresponded to the ratio of the surface saturation concentration N_s^* to the surface atomic density N_s^0 . The growth temperature dependence of the Al composition of the $\text{Al}_x\text{Ga}_{1-x}\text{N}$ epitaxy layers confirmed that the adsorption time τ_c of a MMAI molecule center was larger than the growth time of one atomic layer. The activation energy for surface diffusion Q_d was found to be 0.53 eV.

ACKNOWLEDGMENTS

One of authors (G.S.H.) thanks Shyh-horng Shore of Centre for Nano Science of Technology of National Chiao Tung University for XRD measurements. This work was supported in part by the National Science Council of the Republic of China (ROC) in Taiwan under Contract No. NSC93-2120-M-009-006 and by the Academic Excellence Program of the ROC Ministry of Education under Contract No. NSC93-2752-E-009-008-PAE.

- ¹N. Maeda, T. Saitoh, K. Tsubaki, T. Nishida, and N. Kobayashi, *Jpn. J. Appl. Phys., Part 2* **38**, L987 (1999).
- ²M. A. Khan, X. Hu, A. Tarakji, G. Simin, J. Yang, R. Gaska, and M. S. Shur, *Appl. Phys. Lett.* **77**, 1339 (2000).
- ³T. Takano, Y. Narita, A. Horiuchi, and H. Kawanishi, *Appl. Phys. Lett.* **84**, 3567 (2004).
- ⁴J. Han *et al.*, *Appl. Phys. Lett.* **73**, 1688 (1998).
- ⁵V. Adivarahan, W. H. Sun, A. Chitnis, M. Shatalov, S. Wu, H. P. Maruska, and M. A. Khan, *Appl. Phys. Lett.* **85**, 2175 (2004).
- ⁶M. Shatalov, A. Chitnis, A. Koudymov, J. P. Zhang, V. Adivarahan, G. Simin, and M. A. Khan, *Jpn. J. Appl. Phys., Part 2* **41**, L1146 (2002).
- ⁷G. Sun, R. A. Soref, and J. B. Khurgin, *Superlattices Microstruct.* **37**, 107 (2005).
- ⁸A. V. Kondratyev, R. A. Talalaev, W. V. Lundin, A. V. Sakharov, A. V. Tsatsul'nikov, E. E. Zavarin, A. V. Fomin, and D. S. Sizov, *J. Cryst. Growth* **227**, 420 (2004).
- ⁹T. G. Mihopoulos, V. Gupta, and K. F. Jensen, *J. Cryst. Growth* **195**, 733 (1998).
- ¹⁰S. C. Choi, J. H. Kim, J. Y. Choi, K. J. Lee, K. Y. Lim, and G. M. Yang, *J. Appl. Phys.* **87**, 172 (2000).
- ¹¹R. A. Logan, S. N. G. Chu, M. Geva, N. T. Ha, and C. D. Thurmond, *J. Appl. Phys.* **79**, 1371 (1996).
- ¹²G. S. Huang, X. H. Tang, B. L. Zhang, and S. C. Tjin, *J. Appl. Phys.* **94**, 4890 (2003).
- ¹³W. K. Cho, D. H. Choi, and M.-U. Kim, *Int. J. Heat Mass Transfer* **42**, 4143 (1999).
- ¹⁴J. H. deBoer, *The Dynamical Character of Adsorption*, 2nd ed. (Clarendon, Oxford, 1968).